
HyperJump: Accelerating HyperBand via Risk Modelling

Pedro Mendes¹, Maria Casimiro^{1,2}, Paolo Romano¹

¹*INESC-ID and Instituto Superior Técnico, Universidade de Lisboa*

²*Institute for Software Research, Carnegie Mellon University*

Abstract

In the literature on hyper-parameter tuning, a number of recent solutions rely on low-fidelity observations (e.g., training with sub-sampled datasets or for short periods of time) to extrapolate good configurations to use when performing full training. Among these, HyperBand is arguably one of the most popular solutions, due to its efficiency and theoretically provable robustness

In this work, we introduce HyperJump, a new approach that builds on HyperBand’s robust search strategy and complements it with novel model-based risk analysis techniques that accelerate the search by *jumping* the evaluation of low risk configurations, i.e., configurations that are likely to be discarded by HyperBand. We evaluate HyperJump on a suite of hyper-parameter optimization problems and show that it provides over one-order of magnitude speed-ups on a variety of deep-learning and kernel-based learning problems when compared to HyperBand as well as to a number of state of the art optimizers.

1 Introduction

Hyper-parameter tuning is a crucial phase to optimize the performance of machine learning (ML) models, which is notoriously expensive given that it typically implies repeatedly training models over large data sets. State of the art solutions address this issue by exploiting cheap, low-fidelity models (e.g., trained with a fraction of the available data) to extrapolate the quality of fully trained models.

HyperBand [20], henceforth referred to as HB, is probably one of the most popular solutions in this area. HB is based upon a randomized search procedure, called Successive Halving (SH) [16], which operates in stages of fixed “budget” (e.g., training time or training set size): at the end of stage i , the best performing $1/\eta\%$ configurations are selected to be evaluated in stage $i + 1$, where they will be allocated $\eta \times$ larger budget. By restarting the SH procedure over multiple, so called, brackets using different initial training budgets, HB provides theoretical guarantees of convergence to the optimum, incurring negligible computational overheads and outperforming state of the art optimizers (e.g., based on Bayesian Optimization (BO) [7]) that do not exploit low-fidelity observations. However, the random nature of HB also inherently limits its efficiency, as shown by recent model-based multi-fidelity approaches [14, 17].

In this work, we introduce HyperJump (HJ), a novel hyper-parameter optimization method that builds upon HB’s robust search strategy and accelerates it via an innovative, model-based technique. In a nutshell, the idea at the basis of HJ is to “jump” (i.e., skip either partially or entirely) some of HB’s stages. To minimize the risks associated with jumps, while maximizing the attainable gains by favoring earlier jumps, HJ exploits, in a synergistic way, the following new mechanisms:

- A novel modelling technique to predict the risk of jumping, which we call Expected Accuracy Reduction (EAR). The EAR exploits the model’s uncertainty in predicting the quality of untested configurations as a basis to estimate the expected reduction in accuracy

between **(i)** the best configuration included in the stage reached after a jump and **(ii)** the best configuration discarded due to the jump.

- A criterion for selecting the configurations to include in the HB stage targeted by a jump, which aims to minimize the jump’s risk. This is a combinatorial problem¹, which we tackle via a lightweight heuristic that has logarithmic complexity with respect to the number of configurations in the target stage of the jump.
- A method for prioritizing the testing of configurations in a stage that aims to increase the likelihood of jumping, by favouring the sampling of configurations that are expected to yield the highest reduction of the risk of future jumps.

From a pragmatical perspective, HJ exploits three additional optimizations aimed at enhancing its effectiveness and computational efficiency: **i**) HJ dynamically switches between Gaussian Processes (GPs) and Decision Trees (DTs), so as to achieve the best of both worlds, i.e., higher accuracy when data is scarce and fast training times with large training sets; **ii**) when testing a configuration c with a budget b , the information regarding the quality of c in smaller (untested) budgets b' is extracted, at no extra cost, and fed to the models to enhance their predictive accuracy; **iii**) analogously, albeit symmetrically, when a configuration c is tested on a given budget b , we checkpoint the resulting model and re-use it to accelerate future tests of c that use larger budget values.

We compare HJ with a number of state of the art optimizers [20, 17, 26, 14] on a suite of hyper-parameter optimization problems and show that HJ provides over one-order of magnitude speed-ups on a variety of deep-learning and kernel-based learning problems. We also conduct an ablation study that sheds light on the contributions of the various mechanisms employed by HJ on its performance.

The remainder of this paper is structured as follows. Sec. 2 discusses related work. HJ is presented in Sec. 3 and evaluated in Sec. 4. Sec. 5 concludes this work and discusses its broader impact.

2 Related Work

Existing hyper-parameter techniques can be coarsely classified along two dimensions: i) whether they use model-free or model-based approaches, and ii) whether they exploit solely high-fidelity (i.e., full-training) evaluations or also multi-fidelity ones.

As already mentioned, HB is arguably the most prominent model-free approach at the moment. Its random nature, combined with its SH-based search algorithm, make it not only provably robust, but also very competitive and lightweight when compared to several model-based approaches.

As for the model-based approaches, recent literature on hyper-parameter optimization has been dominated by Bayesian Optimization (BO) [7] methods. BO relies on modelling techniques (e.g., Gaussian Processes [24], Random Forests [6] or TPE [3]) to build a surrogate model of the function $f : \mathcal{X} \rightarrow \mathcal{R}$ to be optimized. The surrogate model is then used to guide the selection of the configurations to test via an *acquisition function* that tackles the exploration-exploitation dilemma. A common acquisition function is the Expected Improvement (EI) [23], which exploits information of the model’s uncertainty on an untested configuration c to estimate by how much c is expected to improve over the current incumbent.

Swerzky et al. [27] were probably the first to propose an adaptation of the BO framework to take advantage of low-fidelity evaluations obtained using a training set of smaller dimensions. This idea was extended in Fabolas [17], which learns the lowest-fidelities that provide more knowledge about the optimum. A related body of work [28, 12, 10, 15] uses models (typically GPs) to predict the loss of a neural network as a function of both the hyper-parameters and the training iterations. Models are then used to extrapolate the full-training loss and cancel under-performing training runs.

From a methodological perspective, the fundamental difference between HJ and this body of model-based works lies in the type of problems that are addressed by their modelling techniques. Since HJ builds on HB’s search strategy, it uses models to answer a relatively simple question: quantify the risk of discarding high quality configurations by accelerating one or more HB stages. The above mentioned works, conversely, being solely model based, need to employ sophisticated modelling techniques to answer complex questions, such as selecting the cheapest configuration to test in order

¹The number of candidate configuration sets for a jump to a stage with k configurations from a stage with n configurations is $\binom{n}{k}$.

Algorithm 1 Pseudo-code for a HJ bracket consisting of S stages, with budget b for the initial stage.

```

1: Set⟨Config⟩  $C = \text{GET\_CONFIGS\_FOR\_BRACKET}()$             $\triangleright \text{Model-driven bracket warmstart (§ 3.4)}$ 
2: Set⟨Config⟩  $T = \emptyset$ ; Set⟨Config⟩  $U = C$ ;            $\triangleright T \text{ and } U \text{ contain the tested/untested configs, resp.}$ 
3: for  $s \in \{0, \dots, S-1\}$  do                                 $\triangleright s \text{ denotes the current stage}$ 
4:   bool  $\text{jump} = \text{false}$ ;
5:   while  $U \neq \emptyset$  do                                 $\triangleright \text{Test configs. in curr. stage, or jump to a future stage}$ 
6:      $\langle \text{target}, \mathcal{S} \rangle = \text{EVALUATE\_JUMP\_RISK}(s, T, U)$             $\triangleright \text{HJ risk-analysis (§ 3.2)}$ 
7:     if  $\text{target} \neq s$  then                                 $\triangleright \text{Jump to target stage}$ 
8:        $s = \text{target}; T = U = \emptyset; C = \mathcal{S}; \text{jump} = \text{true}; \text{break};$ 
9:     else
10:       $c = \text{NEXT\_CONF\_TO\_TEST}(U, b\eta^s)$ ;            $\triangleright \text{Next selected config. minimizes future risk (§ 3.3)}$ 
11:       $\text{acc} = \text{evaluate\_config}(c, b_s)$             $\triangleright \text{Measure config. } c \text{ with budget } b_s \text{ and return its accuracy}$ 
12:       $T = T \cup \{c\}; U = U \setminus \{c\}$ 
13:       $\text{update\_model}(\langle c, b_s, \text{acc} \rangle)$ 
14:    if  $\neg \text{jump}$  then                                 $\triangleright \text{Use HB's policy if HJ did not trigger a jump by the end of the stage}$ 
15:       $U = C = \text{topK}(C, |C|\eta^{-1})$             $\triangleright \text{test top } 1/|\eta| \% \text{ configs. in next stage}$ 

```

to maximize the information gain on the optimum [17, 27] or what is the earliest epoch in which a given train run can be deemed sub-optimal and terminated. By using models to address such complex questions, these techniques require computationally expensive implementations, which impose significant overhead (§ 4). They are also inherently vulnerable to the fallacies of the underlying models in fitting the objective function, due, e.g., to its unknown smoothness or noisy observations. By taking advantage of the (theoretically provable) robustness of HB, which HJ accelerates in a risk-aware fashion via model-driven techniques, we argue that HJ takes the best of both worlds: it preserves HB’s theoretical robustness (§ 3.6), while accelerating it by more than one order of magnitude via the use of models that, being designed to solve a simpler problem, are both more effective and more lightweight than the ones used in previous works (as we will show experimentally).

The works more closely related to HJ are the approaches like BOHB [14, 29, 4] that extend HB with BO to warm start it, i.e., to select (a fraction of) the configurations to include in a new HB bracket. This idea is complementary to the techniques used by HJ to accelerate HB. In fact, HJ incorporates this idea, while revisiting it by proposing an alternative modelling strategy that aims at improving extrapolation across different fidelities. As we show experimentally, when used in combination with this technique, HJ provides more than one order of magnitude speed-ups when compared to BOHB.

3 HyperJump

As already mentioned, a HB bracket is composed of up to S_{\max} stages, where $S_{\max} = \lfloor \log_\eta(R) \rfloor$. R is the maximum “budget” allocated to the evaluation of a hyper-parameter configuration and η is an exponential factor (typically 2 or 3) that controls the increase/decrease of the allocated budget/number of tested configurations in two consecutive stages of the same bracket.

The pseudo-code in Alg. 1 overviews the various mechanisms employed by HJ to accelerate a single HB bracket composed of $S < S_{\max}$ stages. The bracket’s initial stage allocates a budget b , where $b = R\eta^{-(S-1)}$, as prescribed by HB. HJ leverages two main mechanisms to accelerate the execution of a HB bracket, which are encapsulated in the functions EVALUATE_JUMP_RISK and GET_NEXT_CONFIG_TO_TEST.

EVALUATE_JUMP_RISK is executed within the HB’s inner loop (Alg. 1, line 6), in order to decide whether to stop testing of configurations in the current stage and jump to a later stage. This function takes as input the current stage, s , and the configurations already and still to be tested, T and U s. It returns the pair $\langle \text{target}, \mathcal{S} \rangle$ where target denotes the stage to jump to (in which case $\text{target} \neq s$) and \mathcal{S} the selected configurations for the target stage. We detail this function in § 3.2.

In case the risk of jumping is deemed too high, HJ continues testing the configurations in the current stage. Unlike HB, which uses a random order of exploration, HJ prioritizes the order of exploration via the NEXT_CONF_TO_TEST function (Alg. 1 line 10). This function seeks to identify a configuration whose evaluation will lead to a large reduction of the risk of jumping, so as to favour early jumps and enhance the efficiency of HJ. We discuss how we implement this function in § 3.3. After testing configuration c in budget b_s and measuring its accuracy acc , we update the models used to predict the

accuracy of untested configurations (with different budgets). We discuss the type of models used by HJ in § 3.1. Finally, `GET_CONFIGS_FOR_BRACKET` (Alg. 1 line 1) encapsulates the model’s logic to select the configurations to be included in a new bracket, which we detail in § 3.4.

3.1 Predicting the quality of hyper-parameter configurations

HJ’s risk analysis methodology relies on black-box models that can estimate the accuracy of a configuration c in budget b via a Gaussian distribution with parameters (μ, σ) , where μ is the expected value of c ’s accuracy and σ describes the model’s uncertainty. These assumptions are typically met by employing either GPs [24] or ensemble methods [5], e.g., Random Forests [6]. The two have complementary pros and cons: GPs have appealing features with small data sets (e.g., in the early stage of the optimization process, when only a handful of configurations have been tested), where their ability to incorporate prior knowledge via smooth kernel leads to good extrapolation. In GPs, though, training time grows cubically with the number of observations [24], which makes them inherently non-scalable. This efficiency issue can be avoided by using ensembles of scalable learners like decision trees (DTs), whose individual predictions can be used to fit a Gaussian distribution. On the down side, ensemble methods typically generate diverse training sets for the individual learners by “hiding” different subsets of the original data set — which makes these methods inherently more data hungry than GPs.

In HJ, we tackle this problem by using a hybrd approach: we use GPs in the initial stage of the exploration, where these can still be trained efficiently, and switch to an ensemble of decision trees when we have gathered sufficient data to use the latter method effectively. We verified that the training times of our GPs’ implementation (we use the George package [2]) grow significantly with data sets containing more than 100 observations, so we use this threshold to switch to the ensemble method.

As for the feature space used by our models, we include in it, besides the hyper-parameter’s space, also the budget. This enables the learners to extrapolate the quality of configurations based on observations performed using diverse budget levels. Further, it allows us to employ a custom kernel (when using GPs) that encodes the expectation that the loss function has an exponential decay with larger budgets (along with a generic Matérn 5/2 kernel, used to capture relations among the hyper-parameters).

3.2 Deciding whether to jump

We address the problem of deciding whether to adopt HB’s default policy or skip some, or even all of, the future stages of the current bracket by decomposing it into three simpler sub-problems: **1**) modelling the risk of jumping from the current stage to the next stage while retaining an arbitrary subset \mathcal{S} of the configurations C in the current stage (§ 3.2.1); **2**) identifying, in an efficient way, “good” candidates for the subset of configurations to retain after a jump from stage s to stage $s+1$, i.e., configurations that, if included in the target stage of the jump, reduce the risk of jumping (§ 3.2.2); **3**) generalizing the risk modelling to jumps that skip an arbitrary number of stages (§ 3.2.3).

3.2.1 Modelling the risk of jumping to the next stage

Let us start by discussing how we model the risk of jumping from a source current stage s to a target stage, t , that is the immediate successor of s ($t = s + 1$). Denote with C the configurations in s ; with T and U the tested/untested configurations in s , resp., and with \mathcal{S} and \mathcal{D} the subset of configurations in C that are selected/discard, resp., when jumping to stage t .

Our modelling approach is based on the observation that short-cutting HB’s search process and jumping to the next stage exposes the risk of discarding the configuration that achieves maximum accuracy in the current stage (and that may turn out to improve the current incumbent, when tested in full-budget). This risk can be modelled as the difference between two random variables:

$$\mathcal{A}_s^{\mathcal{D}} = \max_{c_i \in \mathcal{D}} A(c_i, b_s), \quad \mathcal{A}_s^{\mathcal{S}} = \max_{c_k \in \mathcal{S}} A(c_k, b_s)$$

defined as the maximum accuracy of the configurations in the set of discarded and selected configurations, respectively. One can then quantify the “absolute” risk of a jump from stage s to stage $s + 1$, which we call Expected Accuracy Reduction (EAR) (Eq. (1)), as the expected value of the difference of these two variables, restricted to the scenarios in which configurations with higher accuracy are discarded due to jumping (i.e., $\mathcal{A}^{\mathcal{D}} - \mathcal{A}^{\mathcal{S}} > 0$):

$$EAR_s^{s+1}(\mathcal{D}, \mathcal{S}) = \int_{-\infty}^{+\infty} x P(\mathcal{A}_s^{\mathcal{D}} - \mathcal{A}_s^{\mathcal{S}} = x) \max\{\mathcal{A}_s^{\mathcal{D}} - \mathcal{A}_s^{\mathcal{S}}, 0\} dx = \int_0^{+\infty} x P(\mathcal{A}_s^{\mathcal{D}} - \mathcal{A}_s^{\mathcal{S}} = x) dx \quad (1)$$

The EAR is computed as follows. The configurations in \mathcal{D} and \mathcal{S} are either untested or already tested. In the former case, we model their accuracy via a Gaussian distribution (given by our predictors); in the latter case, we model their accuracy either as a Dirac function (assuming noise-free measurements, which is the HJ’s default policy) or via a Gaussian distribution (whose variance can be used to model noisy measurements). Either way, the PDF and CDF of $\mathcal{A}^{\mathcal{D}}$ and $\mathcal{A}^{\mathcal{S}}$ can be computed in closed form. However, computing the difference between these two random variables requires solving a convolution that cannot be determined analytically. Fortunately, both this convolution and the outer integral in Eq. (1) can be computed in a few msecs using open source numerical libraries (§ 4.1). Additional details on the computation of the EAR are provided in the supplemental material.

Next, we introduce the rEAR (relative EAR), which is obtained by normalizing the EAR by the loss of the current incumbent, noted l^* : $rEAR_s^{s+1}(\mathcal{D}, \mathcal{S}) = EAR_s^{s+1}(\mathcal{D}, \mathcal{S})/l^*$. The rEAR estimates the “relative” risk of a jump and can be interpreted as the percentage of the maximum potential for improvement that is expected to be sacrificed by a jump. In HJ, we consider a jump “safe” if its corresponding rEAR is below a threshold λ , whose default value we set to 10%. As we will show in the supplemental material, in practical settings, HJ has robust performances for a large range of (reasonable) values of λ . One advantage of using the rEAR, instead of the EAR as risk metric is that the rEAR allows for naturally adapting the risk propensity of HJ’s logic, making HJ progressively less risk prone as the optimization process evolves and better incumbents are found.

3.2.2 Identifying the safest set of configurations for a jump

Determining the safest subset of configurations to include when jumping to the next stage via naive, enumerative methods would have prohibitive costs, as it would require evaluating the rEAR for all possible subsets \mathcal{S} of size $|C|/\eta$ of the configurations in the current stage s . For instance, assuming $\eta = 3$, $|C| = 81$ and less than half of the configurations in C were tested, the number of distinct target sets for a jump of a single stage is $\binom{81}{27} \approx 2E21$.

We tackle this problem by introducing an efficient, model-driven heuristic that recommends a total of $1+2\lfloor\log_{\eta}|\mathcal{S}|\rfloor$ candidates for \mathcal{S} . The first candidate set, denoted \mathcal{K} is obtained by considering the top $|\mathcal{S}|$ configurations, ranked based on their actual or predicted accuracy depending on whether they have already been tested or not. Next, using \mathcal{K} as a template, we generate $\lfloor\log_{\eta}|\mathcal{S}|\rfloor$ alternative candidate sets by replacing the worst $|\mathcal{S}|/\eta^i$ ($1 \leq i \leq \lfloor\log_{\eta}|\mathcal{S}|\rfloor$) configurations in \mathcal{K} with the best configurations in $C \setminus \mathcal{K}$, ranked using the same criterion used to determine \mathcal{K} . We further generate $\lfloor\log_{\eta}|\mathcal{S}|\rfloor$ alternative candidates, which exploits information on model uncertainty as follows: we replace the worst $|\mathcal{S}|/\eta^i$ configurations in \mathcal{K} , ranked according to their lower confidence bound, and replace them with the configurations in $C \setminus \mathcal{K}$ that have the highest confidence (we use a confidence bound of 90%). Intuitively, this way we remove, from the reference set \mathcal{K} , the configurations that are likely to have the lowest accuracy if the model overestimates their mean, and replace them with the configurations that, although having a low (average) predicted accuracy, have the potential to achieve high accuracy, given the model’s uncertainty.

3.2.3 Generalizing to multi-hop jumps

Alg. 2 shows how to compute the rEAR of a jump that skips $j > 1$ stages from the current stage s . This is done in an iterative fashion by computing the EAR for jumps from stage $s + i$ to stage $s + i + 1$ ($i \in [1, j - 1]$) and accumulating the corresponding rEARs to yield the rEAR of the jump.

At each iteration, the candidate sets for the set \mathcal{S} of configurations to be retained after the jump are obtained via the `GET_CANDIDATES_FOR_S` function (§ 3.2.2). Among these $1+2\lfloor\log_{\eta}|\mathcal{S}|\rfloor$ candidate sets, the one with minimum risk is identified. The process is repeated (replacing C with the candidate set that minimizes the risk of the current jump (line 10), until λ is exceeded, thus seeking to maximize the “jump length”, i.e., the number of stages that can be safely skipped. As such, the computation of the risk of a jump from a stage with $|C|$ configurations and that skips $j > 1$ stages requires $\mathcal{O}(j(1 + \log_{\eta}|C|/\eta))$ EAR evaluations. This ensures the scalability of HJ’s risk analysis methodology even when considering jumps that can skip a large number of stages.

Algorithm 2 Pseudo-code for the EVALUATE_JUMP_RISK function.

```

1: <int s, Set<Config>S> EVALUATE_JUMP_RISK(int s, Set<Config> Tested, Set<Config> Untested)
2: rEAR = 0;  $\mathcal{S} = \emptyset$ ;  $C = \text{Tested} \cup \text{Untested}$ .
3: while  $s < S$  do ▷  $S$ : maximum number of stages
4:   Set<Config> candidates = GET_CANDIDATES_FOR_S(Tested, Untested, s)
5:   minRisk =  $\min_{\mathcal{X} \in \text{candidates}} \text{rEAR}_s^{s+1}(\mathcal{X}, C \setminus \mathcal{X})$ 
6:    $\mathcal{S} = \operatorname{argmin}_{\mathcal{X} \in \text{candidates}} \text{rEAR}_s^{s+1}(\mathcal{X}, C \setminus \mathcal{X})$  ▷  $S$ : Set that minimizes the risk
7:   if  $\text{rEAR} + \text{minRisk} > \lambda$  then return  $\langle s, \mathcal{S} \rangle$  ▷ Return the target stage and the set with selected configs.
8:   else ▷ Try to extend the jump by one hop
9:     rEAR += minRisk; s++
10:     $C = \text{Untested} = \mathcal{S}$ ;  $\text{Tested} = \emptyset$ 
11: return  $\langle s, \emptyset \rangle$  ▷ Jump all stages in the current bracket and start a new bracket

```

3.3 Reducing the risk to jump by prioritizing the evaluation order of configurations

HJ also uses a model-based approach to determine in which order to evaluate the configurations of a stage. This mechanism aims to enhance HJ’s efficiency by prioritizing the evaluations of configurations that are expected to yield the largest reduction of risk for future jumps.

The literature on look-ahead non-myopic BO [30, 8, 19, 18] has already investigated several techniques aimed at predicting the impact of future exploration steps on model-driven optimizers. These approaches typically impose large computational overheads, due to the need of performing expensive “simulations”, i.e., re-training the models to simulate alternative evaluation outcomes, and to their ambition to maximize long-term rewards (in contrast to the greedy nature of typical BO approaches).

In HJ, we intentionally depart from these complex/onerous modelling techniques and adopt a lightweight, greedy heuristic that allows for estimating the impact of evaluating an untested configuration without requiring expensive model re-trains. More in detail, we simulate the evaluation of an untested configuration c by querying the model (without retraining it) and including c in the set of tested configurations (using the model predicted accuracy for c as its ground truth). Next, we execute the EVALUATE_JUMP_RISK function to obtain the updated risk of jumping and the corresponding target stage. We repeat this procedure for all the untested configurations in the stage, and select, as the next to test, the one that enables the longest safest jump. Note that our choice not to re-train the model does introduce an approximation, since, when recomputing Eq. (1), the accuracy of the untested configurations will be predicted using “stale” models. As already mentioned, this approximation is motivated by our design goal of keeping HJ lightweight and scalable. In fact, in our preliminary experimentation, we did not notice significant benefits from the use of more complex/expensive simulation techniques proposed in the recent literature on non-myopic BO [19, 8, 22].

3.4 Selecting the configurations to be included in a new bracket

To further accelerate HB, HJ exploits BO to determine which configurations to include when a new bracket is started. To this end, HJ uses its models to identify which set of configurations maximize the EI when deployed using *full budget* — recall that, as in HB, our aim is to maximize accuracy using the full budget. This allows HJ to leverage prior knowledge, unlike HB, at no considerable extra cost, since no additional models need to be trained nor maintained. As mentioned in § 2, the idea of using BO to warm-start HJ’s brackets is not new [14]. However, HJ revisits this approach and introduces some subtle modelling differences that, improve its practical effectiveness.

A first important difference between HJ and BOHB is the way in which HJ’s models capture variations of the budget. As discussed in § 3.1, in HJ, we include the budget as one of the model’s features; further, we use a custom kernel for GPs that encodes the expectation of exponential decay of the loss function with larger budgets. Conversely, previous works, like BOHB, e.g., train a model per budget and query the model associated with the largest budget that has a sufficient number of observations ($d + 1$ configurations, where d is the number of hyper-parameters to optimize). This prevents the models to extrapolate information across budgets, since the models are unaware of how a configuration’s quality is affected by the budget setting. Further, it also delays the time after which one can query the model to obtain predictions related to the use of full budget, since HB’s successive halving logic tests a relatively small number of configurations using full budget. For instance, using

HB’s default parameters ($\eta = 3$, $S_{max} = 5$) and assuming $d = 6$, BOHB can only start using full budget model during its 5-th bracket, i.e., after selecting more than 128 configurations (the ones included in the first 4 brackets) using models trained with low/intermediate budgets. HJ, analogously to BOHB, also starts using the model after $d + 1$ observations; however, unlike BOHB, in the above considered settings, HJ can use full-budget predictions after testing just 7 configurations.

Further, solutions like BOHB avoid the scalability limitations of GPs by resorting to faster modelling techniques, namely TPE [3]. As we show experimentally in the supplemental material, albeit more efficient than GPs, these methods introduce approximations that can degrade the model’s predictive quality and hinder the efficiency of the optimization process.

3.5 Optimizations

HJ adopts two additional optimizations that aim, resp., at reducing the cost of evaluating configurations that were previously tested with lower budgets — which we call *incremental training* — and increasing, at no extra cost, the information that can be fed to the model — which we call *snapshotting*.

Incremental Training. This technique builds on the observation that in a HB’s bracket, configurations are tested multiple times with increasing budget values. We take advantage of this opportunity by saving the model obtained after evaluating a configuration c with budget b , noted $\mathcal{M}(c, b)$. If later on (in the same or in a different HJ’s bracket), c is tested again with a budget $b' > b$, HJ reloads $\mathcal{M}(c, b)$ and resumes the training from there (thus reducing the “cost” of training from b' to b). It should be noted that the idea of suspending and resuming the training process in the context of hyper-parameter optimization is not new, see, e.g., [28, 15], but to the best of our knowledge this opportunity had not yet been exploited in the context of HB-based optimization methods.

Snapshotting. This technique exploits the observation that in modern ML frameworks, (e.g., Neural Networks trained using the parameter server approach [21]), the model’s validation error is typically monitored (and made available) throughout the training process and not only upon its conclusion. We take advantage of this as follows. Assume that a configuration c , not tested with budget b so far, is requested to be tested with budget $b' > b$ (this is possible, e.g., if we are in bracket whose initial stage has budget b and c had not been tested in previous brackets). In such a case, during the evaluation of c with budget b' , when the training process reaches budget b we take a snapshot of the model’s current accuracy, noted $acc(c, b)$. This allows for extending the models’ dataset with the observation $\langle c, b, acc(c, b) \rangle$, enriching its knowledge base essentially at no additional cost.

3.6 Preserving the theoretical guarantees of HyperBand

An appealing theoretical property of HB is that its exploration policy is guaranteed to be at most a constant factor slower than random search. In order to preserve this property, HJ exploits two mechanisms: **i**) it only allow jumps, independently of their risk, with probability p_J ; **ii**) when selecting the configurations to include in a bracket, fraction p_W is selected uniformly at random.

The former mechanism ensures that, independently of how model mispredictions affect HJ’s policy, there exists a non-null probability that HJ will be prevented from jumping (i.e., deviating from the HB’s policy) in any of the brackets that it executes. The latter mechanism, originally proposed in BOHB [14], ensures that, independently of the model’s behavior, every configuration has a non-null probability of being included in a bracket. We adopt as default value for p_W the same used by BOHB, i.e., 0.7, and use the same value also for p_J .

4 Evaluation

This section evaluates HJ both in terms of the quality of the recommended configurations and of its optimization time. We compare HJ against 5 state-of-the-art optimizers using 6 benchmarks. Then we perform a study to dive into the performance of HJ’s different components.

Benchmarks. Firstly, we consider the (distributed) training of 3 different neural networks (NNs): a Convolutional Neural Network (CNN), a Multilayer Perceptron (MLP), and a Recurrent Neural Network (RNN). These networks were implemented using Tensorflow [1] and trained on the MNIST data set [11] in the AWS cloud. The hyper-parameter space is defined by 6 dimensions: batch size, learning rate, and training mode (sync. vs async.), as well as the number, type, and size of the virtual

machines used for training. This space was discretized and exhaustively explored offline in order to identify the optimum. We used the data set produced via these experiments to benchmark HJ also in a neural architecture search (NAS) scenario, in which one seeks to optimize also the underlying NN architecture by selecting either a CNN, a MLP or an RNN.

Next, we consider Light UNET [25] (trained with the 2017 CCF BDCI data set). The hyper-parameter space spans the following 6 dimensions: batch size, learning rate, momentum, training mode, as well as the type and number of GPUs installed on the machine used for training. Also, in this case we discretized the search space and exhaustively sampled it by training the model in each configuration during 5 hours, and measuring its accuracy periodically.

Finally, we use LIBSVM [9] on the Covertype data set [13] (which we subsampled by $\approx 5 \times$ due to time and hardware constraints). The considered hyper-parameters are the kernel (linear, polynomial, RBF, and sigmoid), γ , and C . In this case we could not exhaustively explore off-line the hyper-parameter space, so the optimum is unknown. Since LIBSVM does not output the model’s accuracy during the intermediate phases of training, with this benchmark we do not employ HJ’s incremental training and snapshotting optimizations (§ 3.5). Additional details on these benchmarks are provided in the supplementary material.

Baselines and experimental setup. We compare HJ against five optimizers: HB, BOHB, Fabolas, standard BO with EI, and Random Search (RS). The last two techniques (EI and RS) evaluate configurations only with the full-budget. The implementation of HJ extends the publicly available code of BOHB, which also provides an implementation of HB. We include the URL to the source code of HJ and to the data sets used to evaluate it in the supplemental material. To evaluate Fabolas, we used its publicly available implementation provided by the authors. All the optimizers were implemented in Python3.6 and deployed on VMs equipped with 16 vCPUs and 16GB of RAM; the underlying cloud compute nodes are equipped with two AMD EPYC 7501 CPUs.

We use the default parameters of BOHB and Fabolas. To test HJ in a broader range of settings, we consider two different values of the η parameter: 2 for CNN, NAS and UNET; 3 for the others. For fairness, when comparing HJ, HB and BOHB, we configure them to use the same η value. We use the default value of 10% for the threshold λ for HJ and include in the supplemental material a study on the sensitivity to the tuning of λ . For the optimizers that use multi-fidelity observations, we use time as the budget in RNN, MLP and UNET, and training set size for the remaining benchmarks.

4.1 Experimental results

Figure 1 reports the average loss as a function of the wall clock time (i.e., training and recommendation time) for all the benchmarks but CNN (that can be found in the supplemental material, but shows similar trends). Overall, in all the benchmarks, HJ provides significant speed-ups with respect to all the baselines to recommend both configurations of reasonable/good quality as well as near optimal ones. The largest speed-ups for recommending good quality solutions are achieved in RNN, UNET, NAS, and CNN, where the gains of HJ with respect to the best baseline (typically HB or BOHB) range from around $20 \times$ to $10 \times$. As for identifying close to optimum configurations, the largest speed-ups against the best baseline are achieved in RNN ($\approx 20 \times$), MLP ($\approx 10 \times$) and UNET ($\approx 2.5 \times$).

In our benchmarks, BOHB provides marginal benefits when compared to HB. As we show in the supplemental material, this is imputable to the limited accuracy of the modelling approach used by BOHB (based on TPE and on a model per budget) which, albeit fast, is not very effective in identifying high quality configurations to include in a new bracket. Fabolas’ performance is hindered by its large recommendation times, which are already on the order of a few minutes in the early stages of the optimization and grow more than linearly: as a consequence, Fabolas suffers from large overheads especially with benchmarks that have shorter training times (e.g. MLP) and, across all benchmarks, in the initial phase of the optimization process (where HJ, BOHB and HB, can evaluate several configurations by the time Fabolas produces its first recommendation). Finally, the limitations of EI, which only uses full-budget sampling, are particularly clear with SVM. Here, training times grow more than linearly with the training set size, i.e., the budget used by the multi-fidelity optimizers, amplifies the speed-ups achievable by using low-fidelity observations w.r.t. the other benchmarks.

Ablation study. Figure 1f shows the result of an ablation study aimed at quantifying the contributions of the various mechanisms employed by HJ. To this end, we report the performance obtained on UNET by four HJ variants obtained by disabling each of the following mechanisms: **(i)** the snapshotting

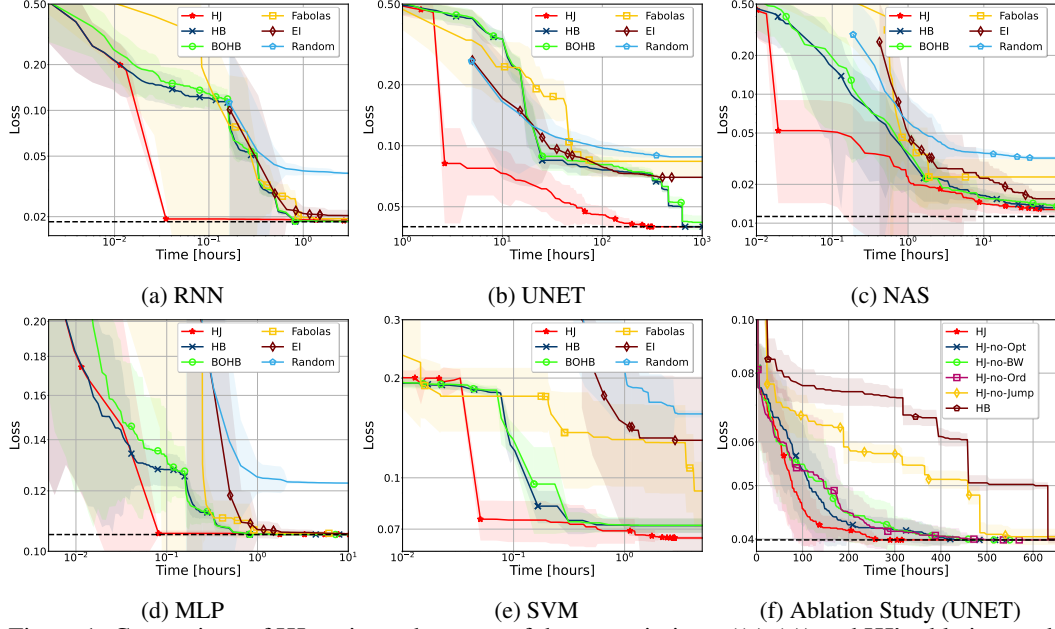


Figure 1: Comparison of HJ against other state of the art optimizers ((a)-(e)) and HJ’s ablation study (f). The dashed horizontal line indicates the optimum (when this is known).

and incremental training optimizations (HJ-no-Opt); **(ii)** warm-starting the bracket (HJ-no-BW); **(iii)** prioritizing the evaluation order of configurations (HJ-no-Ord); **(iv)** the jumping logic (HJ-no-Jump). We include in the plot also HB, which can be regarded as a variant of HJ from which we disabled all of the mechanisms proposed in this paper. On the one hand, this data shows that the first three of these mechanisms have a similar impact on the performance of HJ: disabling any of them increases the time required by HJ to identify the optimum by nearly 40%; a similar slow-down factor can be observed also throughout the optimization process, e.g., the time taken to reach a loss of 5% is around 40% larger with HJ-no-Opt and around 80% larger with HJ-no-BW and HJ-no-Ord. On the other hand, as expected, the largest performance penalty is observed when disabling jumping, which confirms that, as expected, jumping is indeed the mechanism that most contributes to HJ’s efficiency.

Recommendation overhead. We conclude by reporting experimental data regarding the computational overhead incurred by HJ to recommend the next configuration to be tested. The data reported below refer to UNET, but we observed that the overheads do not vary significantly in the other benchmarks. On average, the total recommendation time for HJ is of approx. 0.77 secs, of which: 0.19 secs are spent to train the hybrid GP/DT model; 0.39 secs are spent to determine whether to jump; 0.18 secs are spent to determine the next configuration to test in the current stage. Finally, the computation of the EAR (Eq. (1)) via numerical methods takes on average about 70 msec. Overall, these data confirm the lightweightedness of the proposed solution.

5 Conclusions and Broader Impact

This paper introduces HyperJump, a new approach that complements HB’s robust search strategy and accelerates it by skipping low risk evaluations. HJ’s efficiency hinges on the synergistic use of several innovative risk modelling techniques and of a number of pragmatic optimizations. We show that HJ provides over one-order of magnitude speed-ups on a variety of deep-learning and kernel-based learning problems when compared to HB as well as to a number of state-of-the-art optimizers.

Regarding the broader impact of our work, we argue that HJ can positively impact sustainability of the training pipelines of complex models, which are notorious to have extremely demanding computational and power requirements. Yet, hyper-parameter optimization is a fundamental technique that can be applied to a very broad spectrum of applications, including settings that may have detrimental effects. In the end, HJ’s impact on society is in the hands of those who use it.

References

- [1] M. Abadi et al. Tensorflow: A system for large-scale machine learning. In *Proceedings of OSDI '16: 12th USENIX Symposium on Operating Systems Design and Implementation*, 2016.
- [2] S. Ambikasaran, D. Foreman-Mackey, L. Greengard, D. W. Hogg, and M. O’Neil. Fast direct methods for gaussian processes. *arXiv preprint arXiv:1403.6015*, 2014.
- [3] J. Bergstra, R. Bardenet, Y. Bengio, and B. Kégl. Algorithms for hyper-parameter optimization. In *Advances in Neural Information Processing Systems*, volume 24, pages 2546–2554. Curran Associates, Inc., 2011.
- [4] H. Bertrand, R. Ardon, M. Perrot, and I. Bloch. Hyperparameter optimization of deep neural networks: combining Hperband with Bayesian model selection. In *Proceedings of Conférence sur l’Apprentissage Automatique*, 2017.
- [5] L. Breiman. Bagging predictors. *Machine Learning*, 24(2), 1996.
- [6] L. Breiman. Random forests. *Machine Learning*, 45(1), 2001.
- [7] E. Brochu, V. M. Cora, and N. de Freitas. A tutorial on bayesian optimization of expensive cost functions, with application to active user modeling and hierarchical reinforcement learning. Technical Report arXiv:1012.2599, 2010.
- [8] M. Casimiro, D. Didona, P. Romano, L. Rodrigues, W. Zwanepoel, and D. Garlan. Lynceus: Cost-efficient tuning and provisioning of data analytic jobs. In *Proceedings 20th IEEE International Conference on Distributed Computing Systems*, 2020.
- [9] C.-C. Chang and C.-J. Lin. Libsvm: A library for support vector machines. *ACM Transactions on Intelligent Systems and Technology*, 2, 2011.
- [10] Z. Dai, H. Yu, B. K. H. Low, and P. Jaillet. Bayesian optimization meets Bayesian optimal stopping. In *Proceedings of the 36th International Conference on Machine Learning*, volume 97, 2019.
- [11] L. Deng. The mnist database of handwritten digit images for machine learning research [best of the web]. In *IEEE Signal Processing Magazine*, volume 29. IEEE, 2012.
- [12] T. Domhan, J. T. Springenberg, and F. Hutter. Speeding up automatic hyperparameter optimization of deep neural networks by extrapolation of learning curves. In *Proceedings of the 24th International Joint Conference on Artificial Intelligence*, 2015.
- [13] D. Dua and C. Graff. UCI machine learning repository, 2017.
- [14] S. Falkner, A. Klein, and F. Hutter. BOHB: Robust and efficient hyperparameter optimization at scale. In *Proceedings of the 35th International Conference on Machine Learning*, volume 80, 2018.
- [15] D. Golovin, B. Solnik, S. Moitra, G. Kochanski, J. Karro, and D. Sculley. Google vizier: A service for black-box optimization. In *Proceedings of the 23rd ACM SIGKDD International Conference on Knowledge Discovery and Data Mining*, 2017.
- [16] K. Jamieson and A. Talwalkar. Non-stochastic best arm identification and hyperparameter optimization. In *Proceedings of the 19th International Conference on Artificial Intelligence and Statistics*, 2016.
- [17] A. Klein, S. Falkner, S. Bartels, P. Hennig, and F. Hutter. Fast bayesian optimization of machine learning hyperparamaters on large datasets. In *Proceedings of the 20th International Conference on Artificial Intelligence and Statistics*, volume 54, 2017.
- [18] R. Lam and K. Willcox. Lookahead bayesian optimization with inequality constraints. In *Proceedings of the 31st International Conference on Neural Information Processing Systems*. 2017.

- [19] R. R. Lam, K. E. Willcox, and D. H. Wolpert. Bayesian optimization with a finite budget: An approximate dynamic programming approach. In *Proceedings of the 29th Neural Information Processing Systems Conference*, 2016.
- [20] L. Li, K. Jamieson, G. DeSalvo, A. Rostamizadeh, and A. Talwalkar. Hyperband: A novel bandit-based approach to hyperparameter optimization. *Journal of Machine Learning Research*, 18:1–52, 2018.
- [21] M. Li, D. G. Andersen, J. W. Park, A. J. Smola, A. Ahmed, V. Josifovski, J. Long, E. J. Shekita, and B.-Y. Su. Scaling distributed machine learning with the parameter server. In *Proceedings of the 11th USENIX Conference on Operating Systems Design and Implementation*, 2014.
- [22] P. Mendes, M. Casimiro, P. Romano, and D. Garlan. Trimtuner: Efficient optimization of machine learning jobs in the cloud via sub-sampling. In *2020 28th International Symposium on Modeling, Analysis, and Simulation of Computer and Telecommunication Systems*. IEEE, 2020.
- [23] J. Mockus, V. Tiesis, and A. Zilinskas. The application of bayesian methods for seeking the extremum. In *Toward Global Optimization*, volume 2, pages 117–128. Elsevier, 1978.
- [24] C. E. Rasmussen and C. K. Williams. *Gaussian Processes for Machine Learning*. MIT Press, Cambridge, MA, USA, 2006.
- [25] O. Ronneberger, P. Fischer, and T. Brox. U-net: Convolutional networks for biomedical image segmentation. In *Medical Image Computing and Computer-Assisted Intervention – MICCAI 2015*. Springer International Publishing, 2015.
- [26] J. Snoek, H. Larochelle, and R. P. Adams. Practical bayesian optimization of machine learning algorithms. In *Proceedings of the 25th International Conference on Neural Information Processing Systems*, volume 2, 2012.
- [27] K. Swersky, J. Snoek, and R. P. Adams. Multi-task bayesian optimization. In *Proceedings of the 26th International Conference on Neural Information Processing Systems*, volume 2, 2013.
- [28] K. Swersky, J. Snoek, and R. P. Adams. Freeze-thaw bayesian optimization. *arXiv preprint arXiv:1406.3896*, 2014.
- [29] J. Wang, J. Xu, and X. Wang. Combination of hyperband and bayesian optimization for hyperparameter optimization in deep learning. *arXiv preprint arXiv:1406.3896*, 2018.
- [30] X. Yue and R. A. Kontar. Why non-myopic bayesian optimization is promising and how far should we look-ahead? a study via rollout. *arXiv preprint arXiv:1911.01004*, 2020.

Supplementary Material for HyperJump: Accelerating HyperBand via Risk Modelling

Pedro Mendes¹, Maria Casimiro^{1,2}, Paolo Romano¹

¹*INESC-ID and Instituto Superior Técnico, Universidade de Lisboa*

²*Institute for Software Research, Carnegie Mellon University*

1 Computing the Expected Accuracy Reduction

This section provides details on how to compute the Expected Accuracy Reduction (EAR). Recall that the EAR of a jump from stage s to stage $s + 1$ in which we discard the configurations in \mathcal{D} and select the ones in \mathcal{S} is defined as:

$$EAR_s^{s+1}(\mathcal{D}, \mathcal{S}) = \int_{-\infty}^{+\infty} x P(\mathcal{A}_s^{\mathcal{D}} - \mathcal{A}_s^{\mathcal{S}} = x) \max\{\mathcal{A}_s^{\mathcal{D}} - \mathcal{A}_s^{\mathcal{S}}, 0\} dx = \int_0^{+\infty} x P(\mathcal{A}_s^{\mathcal{D}} - \mathcal{A}_s^{\mathcal{S}} = x) dx \quad (1)$$

where we have noted with $\mathcal{A}_s^{\mathcal{D}} = \max_{c_i \in \mathcal{D}} A(c_i, b_s)$, $\mathcal{A}_s^{\mathcal{S}} = \max_{c_k \in \mathcal{S}} A(c_k, b_s)$.

Before discussing how to compute Eq. (1), let us detail how to compute the PDF of $\mathcal{A}_s^{\mathcal{D}}$ and $\mathcal{A}_s^{\mathcal{S}}$.

Let \mathcal{T} be an arbitrary subset of the configurations in stage s . We use the notation $\phi_{\mathcal{A}_s^{\mathcal{T}}}(x)$ and $\Phi_{\mathcal{A}_s^{\mathcal{T}}}(x)$ to refer to the PDF and CDF, respectively, of $\mathcal{A}_s^{\mathcal{T}}$. We distinguish three cases: (1) \mathcal{T} contains only tested configurations that have been evaluated via noise-free measurements; (2) \mathcal{T} contains only untested configurations or configurations tested via noisy measurements; (3) \mathcal{T} contains some configurations tested via noise-free measurements and configurations that are either untested or tested via noisy measurements

Let us start by considering the first case, i.e., \mathcal{T} only contains configurations tested via noise-free measurements, such that all configurations in \mathcal{T} are described by a Dirac δ function. In this case, the PDF of $\mathcal{A}_s^{\mathcal{T}}$ is simply:

$$\phi_{\mathcal{A}_s^{\mathcal{T}}}(x) = \delta(x - \max_{c_i \in \mathcal{T}} A(c_i, b_s)) \quad (2)$$

If \mathcal{T} only contains untested configurations or if the tested configurations are subject to noisy measurements, then the accuracy predictions for any configuration in \mathcal{T} follow a normal distribution. The CDF of $\mathcal{A}_s^{\mathcal{T}}$, noted $\Phi_{\mathcal{A}_s^{\mathcal{T}}}$, can then be computed in closed form as the product of the CDFs of the normal distributions associated with the configurations $c \in \mathcal{T}$, i.e., $\Phi_{A(c, b_s)}$:

$$\Phi_{\mathcal{A}_s^{\mathcal{T}}}(x) = \prod_{c \in \mathcal{T}} \Phi_{A(c, b_s)}(x) = \prod_{c \in \mathcal{T}} \Phi\left(\frac{x - \mu_{A(c, b_s)}}{\sigma_{A(c, b_s)}}\right) = \exp\left(\sum_{c \in \mathcal{T}} \log \Phi\left(\frac{x - \mu_{A(c, b_s)}}{\sigma_{A(c, b_s)}}\right)\right), \quad (3)$$

where we have denoted with $\Phi(x)$ the CDF of the standard normal distribution and with $\mu_{A(c, b_s)}$, $\sigma_{A(c, b_s)}$ the average and standard deviation of the predicted accuracy of c with budget b_s , respectively. Then, we can determine the PDF by computing the derivative of the CDF:

$$\phi_{\mathcal{A}_s^{\mathcal{T}}}(x) = \frac{d}{dx} \Phi_{\mathcal{A}_s^{\mathcal{T}}}(x) = \prod_{c \in \mathcal{T}} \Phi\left(\frac{x - \mu_{A(c, b_s)}}{\sigma_{A(c, b_s)}}\right) \cdot \sum_{c \in \mathcal{T}} \frac{\phi\left(\frac{x - \mu_{A(c, b_s)}}{\sigma_{A(c, b_s)}}\right)}{\sigma_{A(c, b_s)} \Phi\left(\frac{x - \mu_{A(c, b_s)}}{\sigma_{A(c, b_s)}}\right)} \quad (4)$$

where $\phi(x)$ is the PDF of the standard normal distribution.

Finally, let us consider the case in which \mathcal{T} contains both configurations associated with Gaussian distributions (i.e., untested configurations or tested via noisy measurements) and configurations associated with Dirac δ functions (i.e., tested via noise-free measurements). Let us denote with \mathcal{T}_δ and $\mathcal{T}_{\mathcal{N}}$ the former and latter subset of configurations of \mathcal{T} , respectively. The PDF of $\mathcal{A}_s^{\mathcal{T}}$ is then given by

$$\phi_{\mathcal{A}_s^{\mathcal{T}}}(x) = H(x - \max_{c_i \in \mathcal{T}_\delta} A(c_i, b_s)) \frac{\phi_{\mathcal{A}_s^{\mathcal{T}_{\mathcal{N}}}}(x)}{P_{\mathcal{A}_s^{\mathcal{T}_{\mathcal{N}}}}(x \geq \max_{c_i \in \mathcal{T}_\delta} A(c_i, b_s))} \quad (5)$$

where H is the Heaviside function and $\phi_{\mathcal{A}_s^{\mathcal{T}_{\mathcal{N}}}}(x)$ can be computed using Eq. (4).

Let us now discuss how to compute Eq. (1). The distribution $Z = \mathcal{A}_s^{\mathcal{D}} - \mathcal{A}_s^{\mathcal{S}} = X + Y$ can be computed as the convolution between two random variables X and Y .

$$f_Z(x) = f_X(x) * f_Y(y) = \int_{-\infty}^{+\infty} f_X(k) f_Y(x - k) dk. \quad (6)$$

Hence, Eq. (1) can be computed as:

$$EAR_s^{s+1}(\mathcal{D}, \mathcal{S}) = \int_0^{+\infty} \int_{-\infty}^{+\infty} f_X(k) f_Y(k - x) x dk dx, \quad (7)$$

where f_X and f_Y are obtained by Eq. (4). As an optimization, we take advantage of the existence of tested configurations with noise-free measurements (i.e., associated with Dirac δ functions) in \mathcal{S} and/or \mathcal{D} to simplify Eq. (7) as follows.

If all the configurations in \mathcal{S} are associated with a Dirac δ function and the configurations in \mathcal{D} are all associated with normal distributions, then Eq. (1) can be rewritten as follows:

$$EAR_s^{s+1}(\mathcal{D}, \mathcal{S}) = \int_0^{+\infty} [f_X(x) * f_Y(x)] x dx = \int_0^{+\infty} f_X(x + \max_{c_i \in \mathcal{S}} A(c_i, b_s)) x dx, \quad (8)$$

where f_Y is given by Eq. (2) and $f_X(x)$ by Eq. (4).

Analogously, if all the configurations in \mathcal{D} are tested and modelled by a Dirac δ function (i.e., f_X is determined using Eq. (2)) and \mathcal{S} contains only configurations associated with normal distributions (i.e., $f_Y(x)$ is determined using Eq. (4)), the EAR can be computed as:

$$EAR_s^{s+1}(\mathcal{D}, \mathcal{S}) = \int_0^{+\infty} f_Y(-x + \max_{c_i \in \mathcal{D}} A(c_i, b_s)) x dx \quad (9)$$

Finally, in case only some (but not all) of the configurations in \mathcal{D} or \mathcal{S} are associated with a Dirac δ function, Eq. (7) can be simplified by reducing the interval of integration of the convolution due to the computation of the Heaviside function. For example, if both sets have tested and untested configurations, the EAR can be simplified by

$$EAR_s^{s+1}(\mathcal{D}, \mathcal{S}) = \int_0^{+\infty} \int_M^{+\infty} \frac{\phi_{\mathcal{A}_s^{\mathcal{D}_{\mathcal{N}}}}(k)}{P_{\mathcal{A}_s^{\mathcal{D}_{\mathcal{N}}}}(k \geq \max_{c_i \in \mathcal{D}_\delta} A(c_i, b_s))} \frac{\phi_{\mathcal{A}_s^{\mathcal{S}_{\mathcal{N}}}}(k - x)}{P_{\mathcal{A}_s^{\mathcal{S}_{\mathcal{N}}}}(k - x \geq \max_{c_i \in \mathcal{S}_\delta} A(c_i, b_s))} x dk dx \quad (10)$$

where $M = \max\{\max_{c_i \in \mathcal{D}_\delta} A(c_i, b_s); x + \max_{c_i \in \mathcal{S}_\delta} A(c_i, b_s)\}$

Note that, although the PDF and the CDF of X and Y are known in closed form, the convolution can not be computed analytically (and, as such, neither can Eq. (1)). Therefore, we need to resort to numerical methods to compute the convolution and determine the distribution Z and the respective expected value. Those were implemented in Python3.6 using the function `nquad` of the `scipy` package. Moreover, for efficiency reasons, we implemented in C the function to integrate that is called via the `LowLevelCallable` function. We use the default configuration values of `nquad`, except for the absolute error tolerance (which we set to 1^{-12}) and the upper bound on the number of sub-intervals used in the adaptive algorithm (which we set to 2500).

2 Benchmarks

This section provides additional details on the benchmarks that we used to evaluate HyperJump. Firstly, we deployed in the AWS cloud the distributed training of 3 different neural networks (NNs): a Convolutional Neural Network (CNN), a Multilayer Perceptron (MLP), and a Recurrent Neural Network (RNN). We consider a parameter space composed of 6 dimensions: batch size, learning rate, and training mode, as well as the number, type, and size of the virtual machines used for training. This space was discretized and the considered values are resumed in Table 1.

Table 1: Hyper- and cloud parameters.

Parameter	Values	VM type	VM characteristics	#VMs
Learning rate	$\{10^{-3}, 10^{-4}, 10^{-5}\}$	t2.small	{1 vCPU, 2 GB}	{8,16,32,48,64,80}
Batch size	{16, 256}	t2.medium	{2 vCPU, 4 GB}	{4,8,16,24,32,40}
Training mode	{sync, async}	t2.xlarge	{4 vCPU, 16 GB}	{2,4,8,12,16,20}
		t2.2xlarge	{8 vCPU, 32 GB}	{1,2,4,6,8,10}

We trained the NNs using the MNIST data set [3] with 60000 images to train and 10000 images to test the NN. We trained in each of the different configurations using 5 different sub-sampled data sets and also measured the model’s validation loss periodically. We set an additional timeout to stop the training after 10 minutes in order to control and bound the cost to pay in the cloud. This is a common approach when the training of machine learning (ML) models is deployed in the cloud [6, 1].

We created a variant of the above benchmarks using the training time as budget, instead of data set size. This was done by considering as the full budget a 10 minutes training time; the intermediate time and accuracy values measured when training with the full data set were then used to derive the model’s accuracy at intermediate (time) budgets. We also extended both data sets produced via these experiments in order to benchmark HJ in a neural architecture search (NAS) scenario, in which we also optimize the NN architecture (CNN, MLP, or RNN) by adding an additional dimension to the search space corresponding to the architecture to use.

Next, we considered Light UNET [7] (trained with the 2017 CCF BDCI data set). Also in this case the search space is composed of 6 dimensions/hyper-parameters (see Table 2): batch size, learning rate, momentum, training mode, as well as the type and number of GPUs installed on the machine used for training. Also in this case we discretized the search space and exhaustively sampled it by training the model in each configuration during 5 hours and measuring its accuracy periodically.

In all the benchmarks described so far, in order to reduce noise in the measurements, we trained each configuration three times, monitoring the model’s accuracy periodically, and considered the average of these runs.

Table 2: UNET hyper- and hardware parameters.

Parameter	Values	GPU type	#GPUs
Learning rate	$\{10^{-4}, 10^{-5}, 10^{-6}\}$	GeForce GTX 1080	{1, 2}
Batch size	{1, 2}	GeForce RTX 2080 Super	{1, 2}
Momentum	{0.9, 0.95, 0.99}		
Training mode	{sync, async}		

At last, we considered the training of a Support Vector Machine (SVM) implemented via the LIBSVM [2] framework and trained on the Covertype data set [4]. Due to time and hardware constraints, we reduced the data set size by $\approx 5\times$. In this case, we considered a smaller number of dimensions (i.e., 3 dimensions) but a higher number of configurations. The considered hyper-parameters are the kernel (linear, polynomial with degree from 2 to 4, RBF, and sigmoid), γ , and C . The considered hyper-parameter values are reported in Table 3. Note that in this case we could not exhaustively explore off-line the hyper-parameter space, so the optimum is unknown.

3 Software

HyperJump was implemented based on the public available code of BOHB [5].

Table 3: SVM hyper-parameters.

Parameter	Values
Kernel	{linear, polynomial deg. 2, polynomial deg. 3, polynomial deg. 4, RBF, Sigmoid}
Gamma	{1e-6,1e-5,1e-4,1e-3,5e-3,1e-2,5e-3,0.1,0.5,1,2,5,7,10,20,30,40,50,60,70,80,90,100}
C	{1e-6,1e-5,1e-4,1e-3,5e-3,1e-2,5e-3,0.1,0.5,1,2,5,7,10,20,30,40,50,60,70,80,90,100}

As recommended, we are making the source code of HJ, as well as the data sets used to benchmark it, available for review. Note that while the source code of HJ was submitted as a ZIP file via OpenReview, the data sets are too large to be submitted via OpenReview. We are therefore making them available via this Google Drive link:

<https://drive.google.com/drive/folders/1LaQJrMygNqTYdFZERuwD08Um8t-3vp6s>

Note that we plan to make both HJ’s source code and the data sets used to benchmark it available for the scientific community once the paper is accepted.

4 Supplementary Experimental Results

This section presents supplementary data regarding the comparison of HJ with respect to the set of baseline optimizers described in Sec. 4 of the submitted manuscript.

Figure 1 reports the average loss as a function of the wall clock time (i.e., training and recommendation time) for all the benchmarks used to evaluate HJ. Note that in this figure we are including CNN, which we had to omit from the main body of the paper due to space constraints. In order to ease visualization and comparison among benchmarks, we include in Figure 1 also the benchmarks that were already presented in Figure 1 of our submission.

Through the analysis of the CNN’s data (Figure 1a), we can see that also in this case, analogously to the other benchmarks already discussed in the main body of the paper, HJ provides significant speed-ups both to identify high quality and near optimal configurations. More in detail, HJ reduces the optimization time by approximately $20\times$ to identify a configuration with loss of approximately 2%, and by about $8\times$ to recommend the optimal configuration, when compared to the most efficient baseline (HB).

5 Setting the Threshold

This section reports the result of an experimental study aimed to assess the sensitivity of HJ’s performance to the setting of the threshold λ . We recall that λ is the threshold that HJ uses to decide whether to consider a jump as safe and that 0.1 is its recommended setting.

To this end, we tested HJ on the same set of benchmarks (except SVM, for which we could not conduct this study due to resource constraints) using the following threshold values ($\lambda = \{10^{-3}, 10^{-2}, 10^{-1}, 1\}$) and report the corresponding results in Figure 2.

The key conclusion that can be drawn by analyzing these plots is that the performance of HJ does not vary significantly for values of λ in the $[10^{-1}, 1]$ range, with the best overall performance being achieved when using $\lambda = 10^{-1}$.

We can also observe that the use of the smallest considered threshold settings, i.e., 10^{-2} and 10^{-3} , has a negative impact on the convergence speed of HJ especially in the early stages of the optimization process. At the beginning of the optimization, in fact, models have relatively few available data. As a consequence, models have also higher uncertainty and larger thresholds values need to be employed to allow HJ to shortcut the HB’s search procedure. The effects are particularly noticeable with MLP and RNN, where the use of larger threshold settings (10^{-1} and 1) allows HJ to shortcut almost all of the intermediate stages of the first bracket and to jump to the last (i.e., the full-budget) stage and identify near-optimal configurations.

Overall, in the light of this experimental data, we can conclude that, at least for the benchmarks considered in this study:

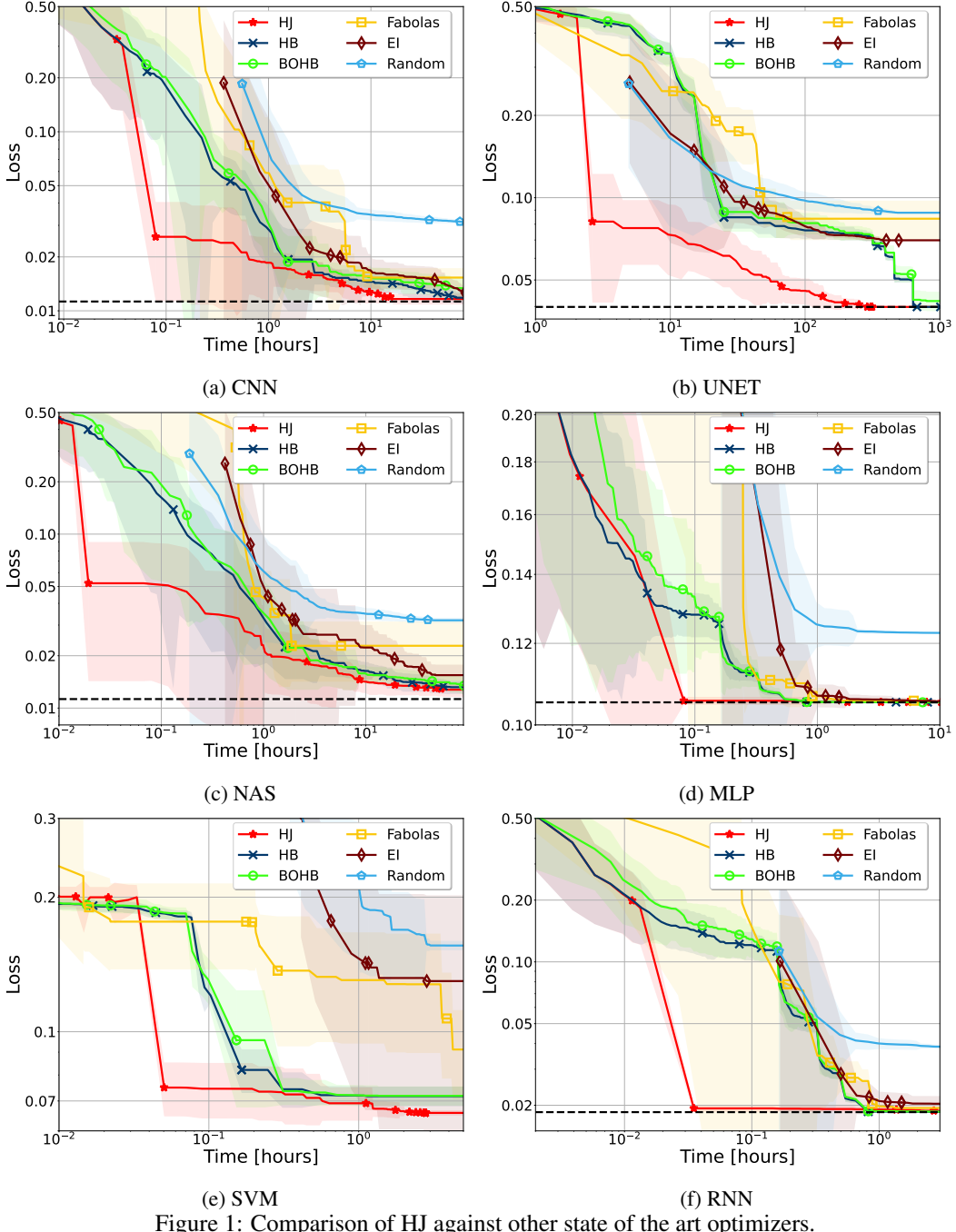


Figure 1: Comparison of HJ against other state of the art optimizers.

1. HJ provides robust performances in a relatively large range of settings for λ (i.e., $\lambda \in [10^{-1}, 1]$).
2. Setting λ below 10^{-1} tends to reduce the effectiveness of HJ by forcing it to adopt overly conservative policies.

6 Bracket Warm Starting

This section aims at evaluating the benefits stemming from using the proposed model-based methodology to warm start a new bracket (i.e., selecting the configurations to be included in a new bracket).

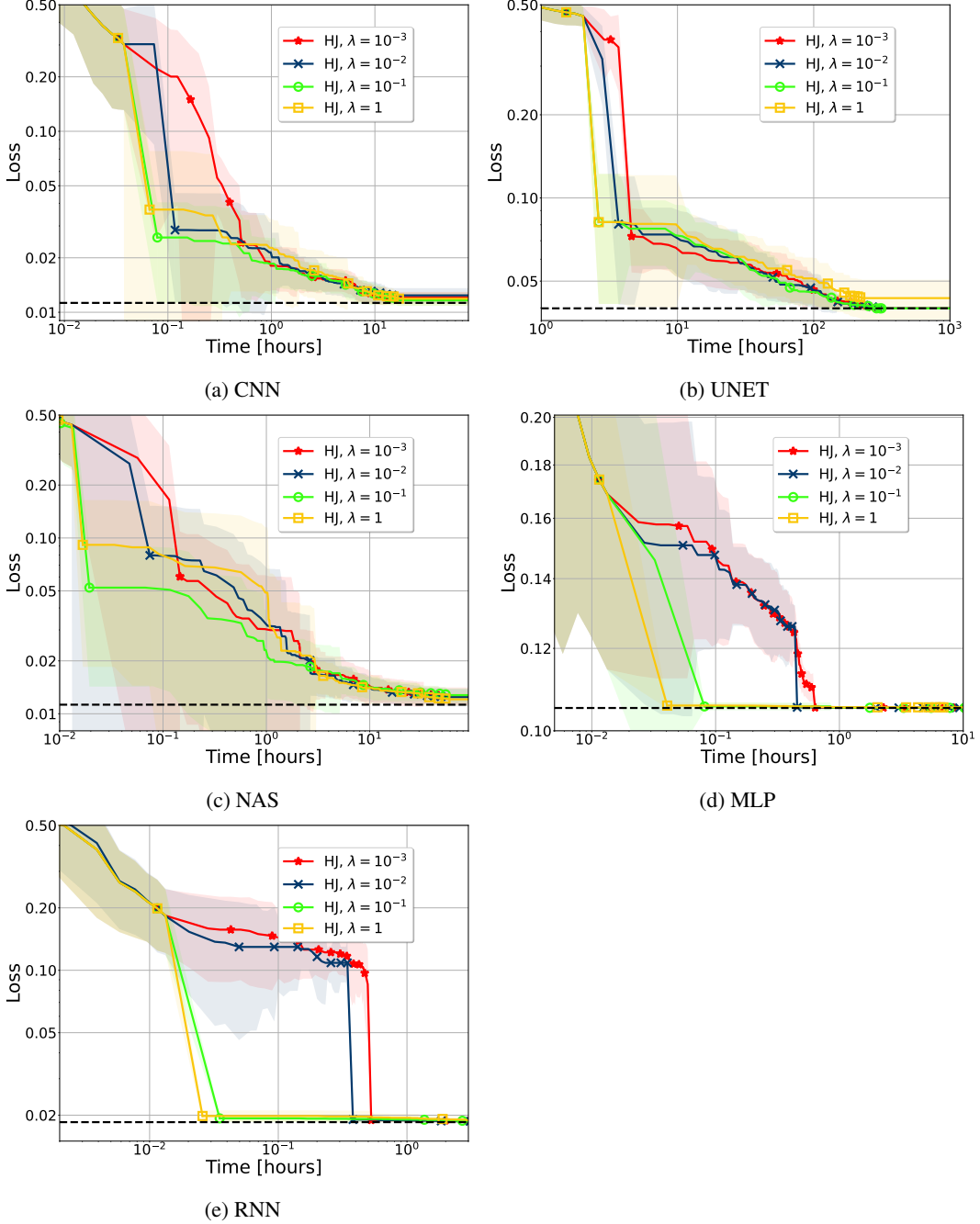


Figure 2: Performance of HyperJump when using different thresholds values across several benchmarks.

To this end we report in Figure 3 the results of an experimental study, based on CNN, in which we compare the following solutions:

- HB, which selects the configuration to include in a bracket uniformly at random.
- BOHB, which uses the Tree Parzen Estimator (TPE) to approximate EI and that employs an independent model per budget. Note that we use the official implementation of BOHB and its default settings. As such, 30% of the configurations are selected uniformly at random.

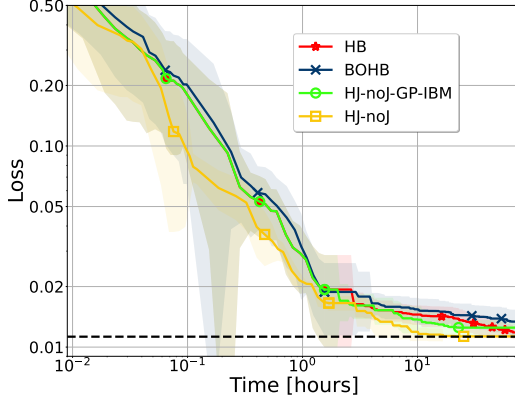


Figure 3: Comparison between different bracket warm starting techniques using CNN.

- A variant of HJ that uses EI and GP as the base learner and employs an independent model per budget (similarly to BOHB). We refer to this baseline as HJ-noJ-GP-IBM in Figure 3.
- A variant of HJ-noJ that uses EI, the hybrid GP/DT learner as the base learner and employs a single model that incorporates the budget among its features. We refer to this baseline as HJ-noJ in Figure 3.

Note that, in order to focus the study solely on the evaluation of different bracket warm starting techniques, we disabled HJ’s jumping mechanism (by setting the risk threshold, λ to 0) both in the HJ-noJ and HJ-noJ-GP-IBM variants. Recall also that HJ, similarly to BOHB, samples 30% of the configurations uniformly at random to preserve the theoretical properties of HB. We preserve this behavior also in HJ-noJ and HJ-noJ-GP-IBM to ensure a fair comparison with BOHB.

By the plot we can see that the HJ-noJ approach achieves approx. $10\times$ speedups to recommend the optimal configuration, as well as consistent speed-ups throughout the whole optimization process. By comparing HJ-noJ and HJ-noJ-GP-IBM we can also observe that the key factor that contributes to the HJ-noJ’s superior performance is the adoption of a single model that incorporates the budget among its features. This can be concluded by observing that the performances of HJ-noJ-GP-IBM and BOHB are very similar and recalling that the only difference between the two solutions is that the former uses EI, whereas the latter adopts TPE.

7 Recommendation Time

At last, we report the average time necessary for HJ to recommend a configuration. Recall that, in order to generate a recommendation, HJ needs to (1) train the model to incorporate the knowledge deriving from testing a new configuration, (2) compute the risk in order to decide whether to jump or not, and (3) select the next configuration to test.

The time taken by these 3 steps is shown in Figure 4 where we also vary the model used (DTs, GPs, and Hybrid GP/DT models). Recall that the hybrid model employs GPs when there are few observations (less than 100), and switches to DTs above this threshold.

As expected, the training time of GPs increases considerably as the number of observations also increases. When using GPs, we also verified an increase in the model’s querying time in the same order of magnitude of the training time. This provokes a significant rise in the time to compute the risk, since in this phase the models need to be queried multiple times. Conversely, the training and inference time of DTs is significantly smaller as can be directly observed in Figure 4a and, indirectly, in Figure 4b, respectively.

We verified a reduction to approximately $5\times$ in the training time and $2.6\times$ in the time to compute the risk when the hybrid model changes from GPs to DTs (i.e., once we gather 100 observations).

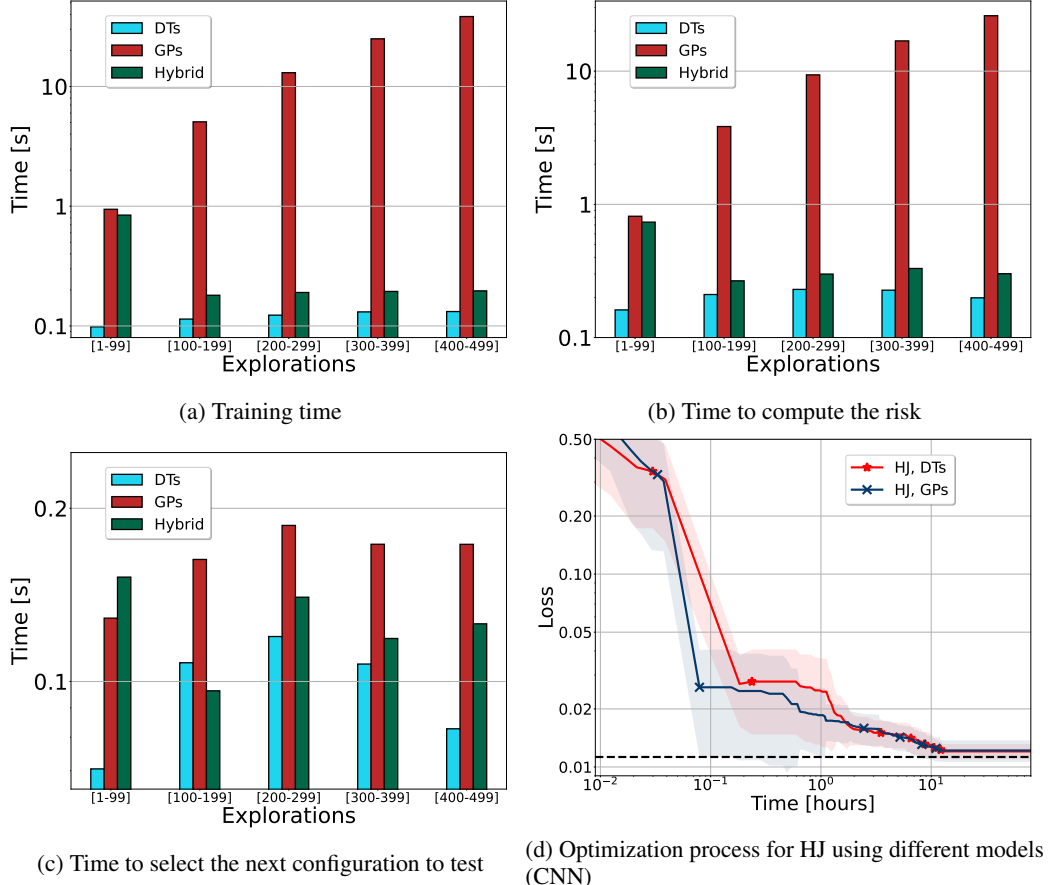


Figure 4: Time to train (4.a), to compute the risk (4.b), and to select the next configuration to test (4.c) using DTs, GPs or the hybrid GP/DT model in CNN. Figure 4.d reports the performance of HJ also in CNN when using DTs and GPs.

In Figure-4c, we can observe that the time to select the next configuration is significantly smaller than the time taken by training and by computing the risk (less than 0.2 seconds, independently of the used model). This is due to the fact that in this phase, we avoid training and querying the model.

Finally, Figure 4d highlights the importance of using GPs (instead of DTs) during the initial stages of the optimization process. To this end, we report the performance of HJ with CNN when using as base model either GPs or DTs. We can clearly observe that the performance of the variant using GPs is significantly better than that of the variant that use DTs during approximately the first two hours of the optimization process. This confirms the superiority of GPs over DTs, as modelling toolkits for optimization problems in case scarce observations are available.

References

- [1] M. Casimiro, D. Didona, P. Romano, L. Rodrigues, W. Zwanepoel, and D. Garlan. Lynceus: Cost-efficient tuning and provisioning of data analytic jobs. In *Proceedings 20th IEEE International Conference on Distributed Computing Systems*, 2020.
- [2] C.-C. Chang and C.-J. Lin. Libsvm: A library for support vector machines. *ACM Transactions on Intelligent Systems and Technology*, 2, 2011.
- [3] L. Deng. The mnist database of handwritten digit images for machine learning research [best of the web]. In *IEEE Signal Processing Magazine*, volume 29. IEEE, 2012.
- [4] D. Dua and C. Graff. UCI machine learning repository, 2017.

- [5] S. Falkner, A. Klein, and F. Hutter. BOHB: Robust and efficient hyperparameter optimization at scale. In *Proceedings of the 35th International Conference on Machine Learning*, volume 80, 2018.
- [6] P. Mendes, M. Casimiro, P. Romano, and D. Garlan. Trimituner: Efficient optimization of machine learning jobs in the cloud via sub-sampling. In *2020 28th International Symposium on Modeling, Analysis, and Simulation of Computer and Telecommunication Systems*. IEEE, 2020.
- [7] O. Ronneberger, P. Fischer, and T. Brox. U-net: Convolutional networks for biomedical image segmentation. In *Medical Image Computing and Computer-Assisted Intervention – MICCAI 2015*. Springer International Publishing, 2015.